JOURNAL OF VIROLOGY, Nov. 1991, p. 6031–6041
0022-538X/91/116031-11$02.00/0

Vol. 65, No. 11

A System for Study of Coronavirus mRNA Synthesis: a Regulated, Expressed Subgenomic Defective Interfering RNA Results from Intergenic Site Insertion

SHINJI MAKINO,* MYUNGSOO JOO, AND JAYNE K. MAKINO

Department of Microbiology, The University of Texas at Austin, Austin, Texas 78712

Received 10 June 1991/Accepted 5 August 1991

A system that exploits defective interfering (DI) RNAs of mouse hepatitis virus (MHV) for deciphering the mechanisms of coronavirus mRNA transcription was developed. A complete cDNA clone of MHV DI RNA containing an inserted intergenic region, derived from the area of genomic RNA between genes 6 and 7, was constructed. After transfection of the in vitro-synthesized DI RNA into MHV-infected cells, replication of genomic DI RNA as well as transcription of the subgenomic DI RNA was observed. S1 nuclease protection experiments, sequence analysis, and Northern (RNA) blotting analysis revealed that the subgenomic DI RNA contained the leader sequence at its 5′ end and that the body of the subgenomic DI RNA started from the inserted intergenic sequence. Two subgenomic DI RNAs were synthesized after inserting two intergenic sites into the MHV DI RNA. Metabolic labeling of virus-specific protein in DI RNA replicating cells demonstrated that a protein was translated from the subgenomic DI RNA, which can therefore be considered a functional mRNA. Transfection study of gel-purified genomic DI RNA and subgenomic DI RNA revealed that the introduction of genomic DI RNA, but not subgenomic DI RNA, into MHV-infected cells was required for synthesis of the subgenomic DI RNA. A series of deletion mutations in the intergenic site demonstrated that the sequence flanking the consensus sequence of UCUAAAC affected the efficiency of subgenomic DI RNA transcription and that the consensus sequence was necessary but not sufficient for the synthesis of the subgenomic DI RNA.

Mouse hepatitis virus (MHV), a coronavirus, is an enveloped virus containing a single-stranded positive-sense RNA genome of approximately 31 kb (13, 14). The virion is composed of four structural proteins, three of which are integral envelope proteins, including the peplomer-forming S (spike) protein, M (membrane) protein and HE (hemagglutinin-esterase) protein. The fourth structural protein, N, is an internal component of the virus. It is a phosphoprotein of 50 kDa (37, 38) and binds to virion RNA (38), forming the helical nucleocapsid of the virion.

In MHV-infected cells seven to eight species of virus-specific subgenomic mRNAs composing a 3′-coterminal nested-set structure (10, 15) are synthesized, and from each of these a viral protein is translated. These subgenomic mRNAs are named mRNAs 1 to 7, according to decreasing order of size (10, 15). mRNA 1 is structurally identical to the genomic RNA which is detected in MHV particles, whereas the other subgenomic mRNAs are not packaged into virions (13, 20). The 5′ end of the MHV genomic RNA contains a 72- to 77-nucleotide-long leader sequence (9, 11, 36). The 3′ region of the leader sequence contains a pentanucleotide sequence, UCUAA, that is repeated two to four times in different MHV strains (19). Downstream of the leader sequence are the MHV-specific genes, each of which is separated by a special short stretch of sequence, the intergenic sequence. All MHV intergenic sequences analyzed so far include the unique consensus sequence of UCUAAAC or a very similar sequence (33). A sequence identical to the leader sequence, of 72 to 77 nucleotides, is also found at the 5′ end of each and every MHV mRNA species, and these leader sequences are fused with the mRNA body sequence which starts from the intergenic site consensus sequence (9, 11, 33, 36). The leader fusion site on a given species of MHV subgenomic mRNA is heterogeneous (22), and that heterogeneity is due to a variation in the number of pentanucleotide (UCUAA) repeats at the leader fusion site (22).

It has been proposed that coronavirus utilizes a unique leader RNA-primed transcription in which a leader RNA is transcribed from the 3′ end of the genome-sized negative-strand template RNA, dissociates from the template, and then rejoins the template RNA at downstream intergenic regions to serve as the primer for mRNA transcription (8). This transcription model is based on the observation that the negative-stranded RNA of MHV is of genomic size (12), and a body of evidence indeed supports this transcription model (1, 2, 8, 23). However, Sethna et al. demonstrated the presence of subgenomic-size negative-stranded RNAs containing the antileader sequence in transmissible gastroenteritis virus and bovine coronavirus-infected cells (30, 31). Also, subgenomic replicative intermediate RNAs corresponding to each MHV subgenomic mRNA species have been demonstrated in MHV-infected cells (29). These recent discoveries cannot be explained by the original leader RNA-primed transcription mechanism. The mechanism of coronavirus transcription remains to be elucidated.

There is a rough correlation between the degree of intergenic site nucleotide homology with the leader sequence and the amount of mRNA transcribed (33). The effect on transcription of both the sequences at the 3′ end of the leader and the intergenic site has been demonstrated by using several recombinant MHVs and mutant MHVs with differing pentanucleotide repetitions (19, 32). These data strongly indicate that the complementary sequences present at the leader RNA and the intergenic site play an essential role(s) in MHV transcription.

* Corresponding author.

TABLE 1. Synthetic oligonucleotides used in this study

Oligonucleotide	Sequence	Binding site[a]	Polarity
7	5′-TTGCCCAGGAACAAAAGA-3′	MHV mRNA 7, 87–104	Negative
52	5′-AAGCTTAATACGACTCACTATAGTATAAGAGTGATTGGCGTCCGTAC-3′	MHV genome, 0–23	Positive
78	5′-AGCTTTACGTACCCTCTCTACTCTAAAACTCTTGTAGTTT-3′	MHV genome, 25–56	Positive
79	5′-AAACTACAAGAGTTTTAGAGTAGAGAGGGTACGTAA-3′	MHV genome, 25–56	Negative
130	5′-TTCCAATTGGCCATGATCAA-3′	DIssE, 2186–2205	Negative
167	5′-CTTCTGGGGATCCTCGTC-3′	MHV genome, 452–469	Negative
963	5′-CAAACGATCGATATCAGAAAGATGAAGTAGA-3′	DIssE, 1752–1769	Positive
1090	5′-TAGATTAGACTCAACAAT-3′	PR6, 3095–4014	Negative
1092	5′-CTAATCTAAACAGGATGTCTT-3′	PR6, 4007–4031	Positive
1093	5′-AAGACATCCTGTTTAGATTAG-3′	PR6, 4007–4031	Negative
1111	5′-GAGCCAGAAGGCTGCGAT-3′	DIssF, 3184–3201	Negative
1112	5′-ATTGTTGAGTCTAATCTA-3′	PR6, 3095–4014	Positive
1115	5′-TCTAGCACGTGGCACTA-3′	DIssF, 3034–3050	Positive
1151	5′-TTAGACTCAACAATGCGG-3′	PR6, 3091–4015	Negative
1152	5′-CATTGTTGAGTCTAAACAGGAT-3′	PR6, 3094–4026	Positive
1153	5′-ATTGTTGAGTCTAAAAGGAT-3′	PR6, 3095–4026	Positive
1154	5′-ATCCTGTTTAGCTCAACA-3′	PR6, 3097–4026	Negative
1155	5′-TGTTGAGCTAAACAGGAT-3′	PR6, 3097–4026	Positive
1177	5′-ATTGTTGAGAATCTAAAC-3′	PR6, 3095–4017	Positive
1178	5′-GTTTAGATTCTCAACAAT-3′	PR6, 3095–4017	Negative
1241	5′-CGCATTGTTGAGTCTAA-3′	PR6, 3092–4015	Positive
1291	5′-TTAAAGTAGATTCTCAAC-3′	PR6, 3098–4023	Negative
1292	5′-GTTGAGAATCTACTTTAA-3′	PR6, 3098–4023	Positive

[a] The oligonucleotide binding site nucleotide numbers for the MHV genome, MHV mRNA 7, DIssE, and DIssF are derived from published data (21, 26, 33–35). Oligonucleotides which bind to positive-sense MHV RNA have negative polarities.

When MHV was serially passaged in tissue culture at a high multiplicity of infection, a variety of defective-interfering (DI) RNAs of different sizes was detected (17, 24, 39). MHV DI RNAs can be classified into three types. One is DIssA RNA of nearly genomic size, which is efficiently packaged into virus particles and replicates itself even in the absence of helper virus infection (17, 20). The second type consists of the smaller DI RNAs, those requiring helper virus infection for replication that are not packaged efficiently into MHV particles (20). The structure and multiplication mechanisms of DIssE RNA, the 2.3-kb prototype of the second DI RNA group, has been studied in detail (18, 20, 21). The third type of DI RNA also requires helper virus infection for its replication; however, it can package efficiently because of the presence of a packaging signal (4, 26). Both the second and third types of DI RNAs contain one large open reading frame from which proteins are translated (21, 26). DIssF RNA, the prototype of the third MHV DI RNA type, is 3.6 kb in size and consists of five noncontiguous genomic regions, including the leader sequence and the 3′ end of the genome. A system was established in which complete cDNA clones of both DIssE and DIssF RNAs are placed downstream of the T7 RNA polymerase promoter to generate DI RNAs capable of extremely efficient replication in the presence of a helper virus. This system has been used for studying MHV RNA replication (18) and analysis of the packaging signal (26). Because of the large size of coronavirus genomic RNA, infectious cDNA is not yet available. Therefore, the MHV DI cDNA system is currently one of the most useful systems for the study of coronavirus multiplication.

In this paper, the establishment of still another MHV DI cDNA system enabling the study of MHV transcription is described. In this system, a subgenomic DI RNA was synthesized from a DI genomic RNA in which an intergenic sequence had been inserted. Site-directed mutagenesis at the inserted intergenic site revealed that the sequences flanking the consensus sequence of UCUAAAC affected the efficiency of subgenomic DI RNA transcription and that the consensus sequence was necessary but not sufficient for the synthesis of the subgenomic DI RNA. The possible mechanism of coronavirus transcription and the usefulness of this system for future studies are discussed.

MATERIALS AND METHODS

Viruses and cells. The plaque-cloned A59 strain of MHV (MHV-A59) was used as a helper virus. Mouse DBT cells (6) were used for growth of viruses.

DNA construction. (i) Construction of PR6 and PR7. The synthetic oligonucleotides used in the present study are listed in Table 1. The procedures for construction of PR6 and PR7 are diagrammed in Fig. 1. In order to introduce the intergenic site downstream of the MHV DI cDNA packaging signal (4, 26), an *Eco*RV restriction site was created downstream of the packaging signal in a DIssF-derived complete cDNA clone. DIssE-specific cDNA clone DE5-w4 (18) was incubated with two oligonucleotides, 963 and 130, at 93°C for 60 s, 37°C for 40 s, and 72°C for 100 s in polymerase chain reaction (PCR) buffer (0.05 M KCl, 0.01 M Tris-hydrochloride [pH 8.0], 0.0025 M $MgCl_2$, 0.01% gelatin, 0.17 mM each deoxynucleoside triphosphate, and 5 U of *Taq* polymerase [Perkin Elmer-Cetus]) for 20 cycles. Oligonucleotide 963 contains *Pvu*I and *Eco*RV sites, and it hybridizes with the antigenomic sense of DE5-w4 at nucleotides 1752 to 1769 from the 5′ end of DIssE cDNA. Oligonucleotide 130 contains an *Msc*I site and hybridizes with DE5-w4 at nucleotides 2186 to 2205 from the 5′ end of the DIssE cDNA sequence. After the reaction, the PCR product was digested with *Pvu*I and *Msc*I, and a 0.46-kb DNA fragment was purified. The 2.0-kb *Spe*I-*Msc*I fragment from the complete cDNA clone of DIssF (DF 1-2 [26]), the 1.6-kb *Spe*I-*Pvu*I fragment of DF 1-2, and the 0.46-kb *Pvu*I-*Msc*I PCR fragment were ligated, yielding plasmid MP 51-2. MHV-A59 genomic RNA was

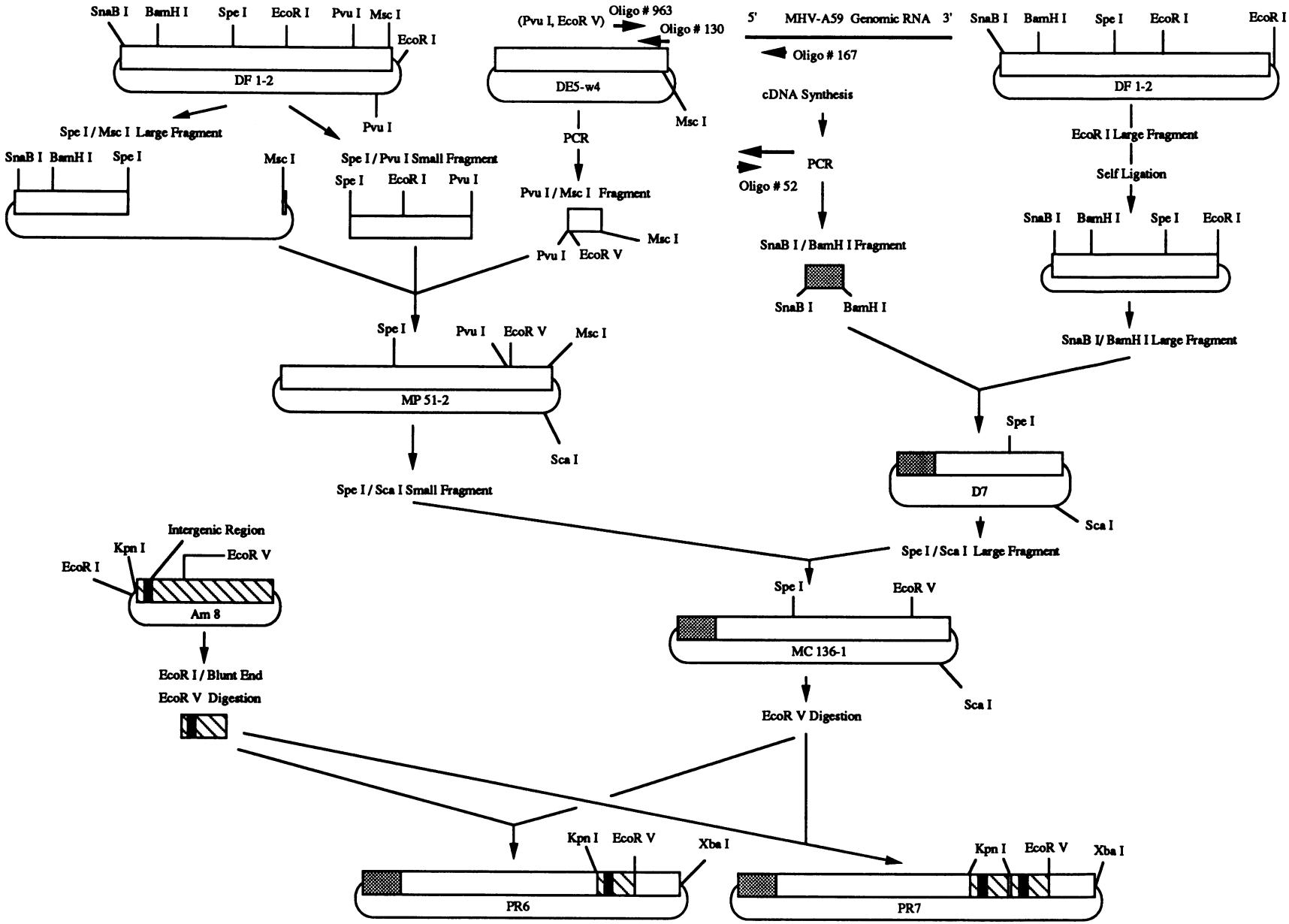

FIG. 1. Construction of the clones, MC 136-1, PR6, and PR7 MHV DI cDNAs. The details of each step are described in Materials and Methods. The open boxes, shaded boxes, and cross-hatched boxes represent sequences derived from the DI cDNA clone, MHV-A59, and clone Am 8 cDNA, respectively. The black boxes indicate the intergenic sequence.

mixed with oligonucleotide 167, which hybridizes with MHV-A59 genomic RNA 452 to 469 nucleotides from the 5′ end, and the cDNA was synthesized as previously described (21). One-fifth of cDNA product was then mixed with oligonucleotide 52 (18) in PCR buffer, and the samples were incubated at 93°C for 30 s, 55°C for 30 s, and 72°C for 100 s for 25 cycles. The PCR product was digested with *Sna*BI and *Bam*HI, and the 0.44-kb *Sna*BI-*Bam*HI fragment was ligated with a cDNA clone containing the 5′ 2.2 kb of DF 1-2 cDNA in a pT 7-4 vector to yield plasmid D7. The 2.6-kb *Spe*I-*Sca*I fragment of MP 51-2 was ligated with the 3.3-kb *Spe*I-*Sca*I fragment of plasmid D7, yielding the MC 136-1 plasmid whose 5′ end 469 nucleotides are derived from MHV-A59. In order to include the intergenic sequence of MHV in the MC 136-1 clone, Am 8, which contains a 1.8-kb cDNA fragment from the 3′ end of MHV-JHM genomic RNA in a pTZ18U vector (18), was digested with *Eco*RI and blunt ended (28). The 559-nucleotide *Eco*RV-*Eco*RI fragment resulting from that digestion was inserted into the *Eco*RV site of MC 136-1, yielding PR6 with its one inserted fragment. Plasmid PR7, which contains two directly repeated inserted fragments, was also obtained from that ligation.

(ii) Construction of mutant DI cDNAs. A procedure based on recombinant PCR was employed for site-directed mutagenesis (5). Oligonucleotide 1115, which hybridizes 622 to 606 nucleotides upstream of the *Eco*RV site of PR6, and oligonucleotide 1111, which hybridizes 105 to 88 nucleotides downstream from the *Eco*RV site of PR6, were used as the outside oligonucleotides. The same PCR conditions, in which plasmid DNA was incubated with two oligonucleotides in PCR buffer at 93°C for 30 s, 37°C for 45 s, and 72°C for 100 s for a total of 25 cycles, were used for the construction of all mutants. The combinations of inside oligonucleotides for the first PCR and the template DNA for each mutant are as follows (in the order name of mutant, oligonucleotides used with oligonucleotide 1111, oligonucleotides used with oligonucleotide 1115, and template DNA): PR6 mutant 1, oligonucleotide 1112, oligonucleotide 1090, PR6 template; PR6 mutant 2, oligonucleotide 1092, oligonucleotide 1093, PR6 template; PR6 mutant 8, oligonucleotide 1112, oligonucleotide 1090, PR6 mutant 2 template; PR6 mutant 3, oligonucleotide 1152, oligonucleotide 1151, PR6 mutant 8 template; PR6 mutant 4, oligonucleotide 1153, oligonucleotide 1151, PR6 mutant 3 template; PR6 mutant 5, oligonucleotide 1155, oligonucleotide 1154, PR6 mutant 3 template; PR6 mutant 9, oligonucleotide 1177, oligonucleotide 1178, PR6 mutant 1 template; PR6 mutant 10, oligonucleotide 1241, oligonucleotide 1151, PR6 mutant 9 template; PR6 mutant 11, oligonucleotide 1292, oligonucleotide 1291, PR6 mutant 9 template.

Each set of the purified first PCR product was then mixed, and the second PCR was performed under the same conditions. The final PCR product was then digested with *Kpn*I and *Eco*RV, and the 0.56-kb *Kpn*I-*Eco*RV PCR fragment was cloned into the 6.0-kb *Kpn*I-*Eco*RV fragment of PR6. The *Kpn*I-*Eco*RV region of each clone was sequenced to confirm the presence of the specific mutation and the absence of other mutation sites.

RNA transcription and transfection. Plasmid DNAs were linearized by *Xba*I digestion and transcribed with T7 RNA polymerase as previously described (18). The cationic lipid lipofection procedure (3) was used for RNA transfection. This basically followed the procedure established by Weiss et al. (40). Briefly, DBT cells in 60-mm-diameter dishes were first infected with MHV-A59. After 1 h of virus adsorption, virus inoculum was removed and cells were washed with prewarmed minimal essential medium (MEM) three times prior to the RNA transfection. The in vitro-synthesized DI RNA which had been incubated with 7.5 μg of lipofectin reagent (Bethesda Research Laboratories) for 15 min at room temperature in 0.5 ml of MEM was added to an MHV-infected culture. After incubation at 37°C for 1 h, 1.5 ml of prewarmed MEM was added and further incubated at 37°C for 1 h. This medium was then replaced with 3 to 5 ml of medium containing MEM, 10% tryptose phosphate broth (Difco), and 2% fetal calf serum and further cultured at 37°C.

Preparation of virus-specific intracellular RNA and agarose gel electrophoresis. Virus-specific RNAs in virus-infected cells were labeled with $^{32}P_i$ as previously described (25). Virus-specific RNA was separated by electrophoresis on 1% agarose gels after denaturation with 1 M glyoxal (27). For preparative gel electrophoresis, RNA was separated on 1% low-melting-point agarose gels without prior treatment with glyoxal (18). The RNA was extracted from the gel slice by the published procedures (18).

Northern (RNA) blotting. Intracellular RNA was adjusted to 2.2 M formaldehyde–50% formamide in MOPS (morpholinepropanesulfonic acid) buffer (20 mM MOPS [pH 7.0], 5 mM sodium acetate, 1 mM EDTA). Samples were heated at 65°C for 5 min and applied to 1% agarose gels in 2.2 M formaldehyde-MOPS buffer. After electrophoresis, the gel was treated with 50 mM NaOH for 20 min and neutralized with 100 mM Tris-hydrochloride (pH 7.2) for 10 min. The gel was then soaked in 20× SSC (1× SSC is 0.15 M NaCl plus 0.015 M sodium citrate) for 10 min. RNA was transferred to Biodyne nylon filters (ICN Radiochemicals) in 20× SSC overnight and dried and baked at 80°C for 2 h. The membrane was prehybridized at 47°C for 4 h in 5× SSC–0.1% Ficoll–0.1% polyvinylpyrrolidone–0.1% bovine serum albumin–50 mM sodium phosphate (pH 7.0)–1% sodium dodecyl sulfate (SDS) containing 100 μg of sheared salmon sperm DNA and 50 μg of tRNA per ml. Oligonucleotide 79 (18), which was 5′ end labeled with [γ-^{32}P]ATP with polynucleotide kinase (28) was denatured at 100°C for 10 min and added to the prehybridization solution, and hybridization was carried out at 47°C for 16 h. The membrane was washed two times at room temperature for 30 min in 2× SSC and then once at 47°C for 30 min in 2× SSC. The membrane was then air-dried and exposed to Kodak XAR-5 film.

S1 nuclease mapping. The gel-purified PR6 subgenomic DI RNA which was obtained from cells infected with passage 1 sample of PR6 DI particles was incubated in 8 μl of distilled water containing 10 mM methyl mercury. After 10 min of incubation at room temperature, the sample was further incubated with oligonucleotide 130 in 50 μl of buffer containing 60 U of RNasin (Promega), 10 mM $MgCl_2$, 100 mM KCl, 50 mM Tris-hydrochloride (pH 8.3 at 42°C), 10 mM dithiothreitol, 1.25 mM (each) dATP, dCTP, and dTTP, 2.4 μM dGTP, 28 mM β-mercaptoethanol, 100 μCi of [α-^{32}P]dGTP (ICN, >3,000 Ci/mmol), and 20 U of avian myeloblastosis virus reverse transcriptase (Promega) at 42°C. After incubation for 40 min, dGTP was added to a final concentration at 1.25 mM and then incubated for an additional 30 min at 42°C. After incubation, the sample was incubated at 100°C for 3 min and then quickly chilled on ice. To remove the RNA template, the sample was incubated with RNase A (20 μg/ml) and RNase T_1 (200 U/ml) for 15 min at 37°C, and then the sample was mixed with an equal volume of a buffer containing 0.2 M Tris-hydrochloride (pH 7.5), 25 mM EDTA, 0.3 M NaCl, and 2% SDS and incubated at 37°C in the presence of proteinase K at final concentration of 200 μg/ml. This primer extension product was extracted twice with phenol-chloro-

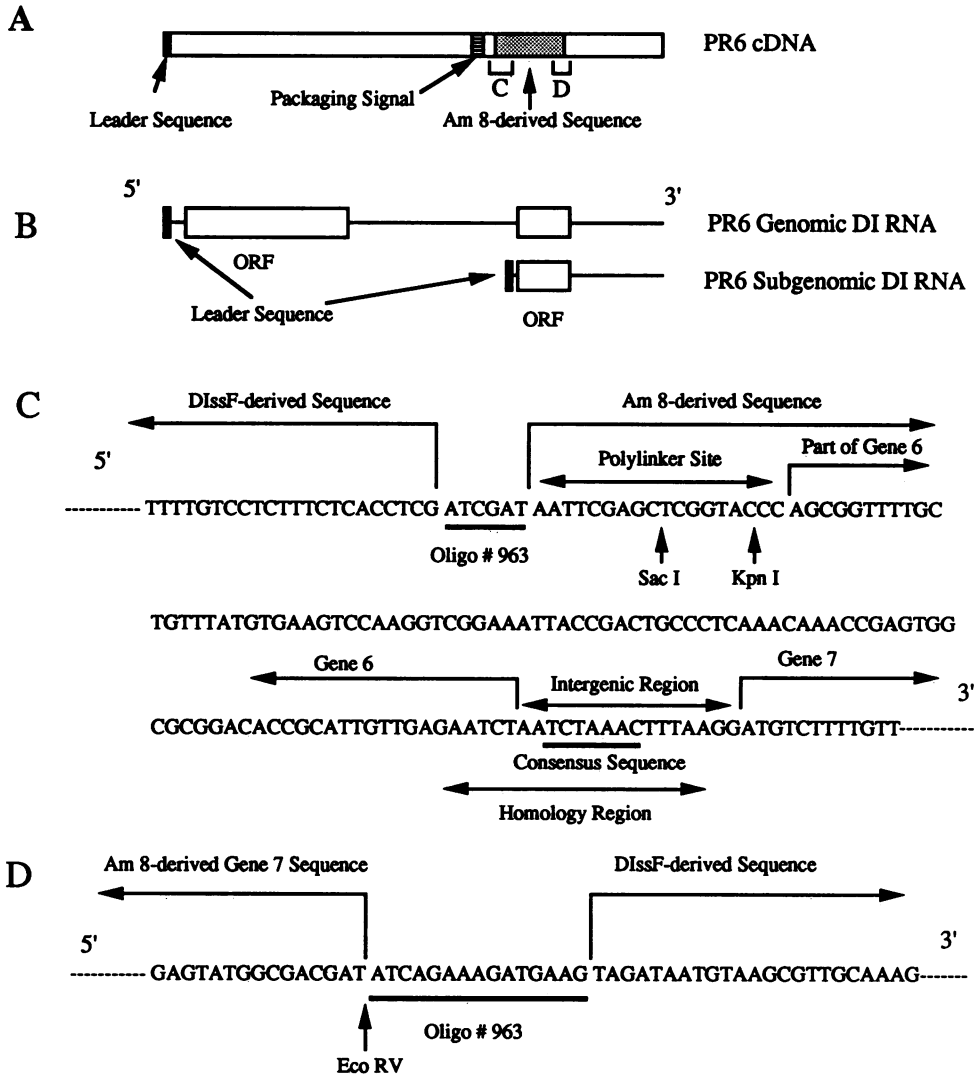

FIG. 2. Diagram of the structure of PR6. (A) The black box, cross-hatched box, and shaded box represent leader sequence, packaging signal, and Am 8-derived sequences, respectively. The identification of a packaging signal will be described elsewhere (4). The sequences corresponding to C and D are shown below. (B) Diagram of the structure of PR6 genomic RNA and PR6 subgenomic RNA. The black boxes and open boxes represent leader sequence and open reading frame, respectively. (C) Sequence at the 5′ boundary of the inserted Am 8-derived fragment and DIssF. (D) Sequence at the 3′ boundary of the inserted Am 8-derived fragment and DIssF.

form and precipitated with ethanol. Full-length cDNA product, purified by gel electrophoresis, was mixed with a gel-purified in vitro-synthesized PR6 genomic DI RNA in 30 μl of a hybridization buffer containing 40 mM PIPES (piperazine-*N*,*N*′-bis [2-ethanesulfonic acid]; pH 6.4), 1 mM EDTA, 0.4 M NaCl, and 80% formamide, and incubated at 85°C for 10 min followed by incubation at 30°C. After 16 h of incubation, 300 μl of ice-cold nuclease S1 buffer (0.28 M NaCl, 0.05 M sodium acetate (pH 4.5), 4.5 mM $ZnSO_4$, 20 μg of single-stranded carrier DNA per ml, and 1,000 U of nuclease S1 (Boehringer Mannheim) per ml was added to the sample and further incubated for 60 min at 37°C. The sample was then chilled at 0°C, and 80 μl of nuclease S1 stop buffer (4 M ammonium acetate, 50 mM EDTA, and 50 μg of tRNA per ml) was added. The sample was then extracted with phenol-chloroform and precipitated with ethanol. Then S1 nuclease-treated cDNA sample was separated by 1.4% agarose gel electrophoresis after denaturation of the sample with glyoxal (27).

In vitro translation. An mRNA-dependent rabbit reticulocyte lysate (Promega) was used as previously described (21, 26, 35).

Labeling of intracellular proteins, immunoprecipitation, and SDS-PAGE. Labeling of intracellular proteins, immunoprecipitations, and SDS-polyacrylamide gel electrophoresis (PAGE) were performed as previously described (26, 41). The passage 1 virus samples were used for the virus inoculum.

RESULTS

Construction of DI RNAs capable of efficient subgenomic DI RNA transcription in the presence of helper virus. To further understand the mechanism of MHV RNA transcription, a

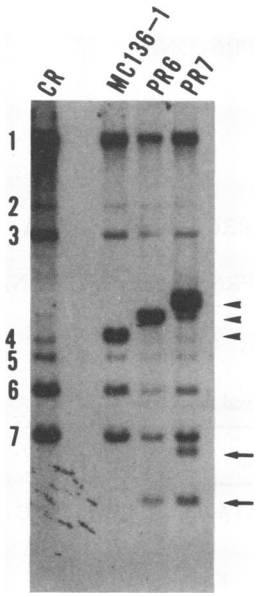

FIG. 3. Synthesis of genomic DI RNA and subgenomic DI RNA species. Virus-specific RNA species were labeled with $^{32}P_i$ for 2 h in the presence of actinomycin D (2.5 μg/ml) at 5 h postinfection. RNAs were denatured with glyoxal and electrophoresed on 1% agarose gels. Passage 1 virus samples were used for inoculum. CR, passage 1 virus obtained from mock-transfected and MHV-A59-infected cells. The MHV specific mRNA species are numbered 1 to 7. DI genomic RNAs and subgenomic DI RNAs are shown by arrowheads and arrows, respectively.

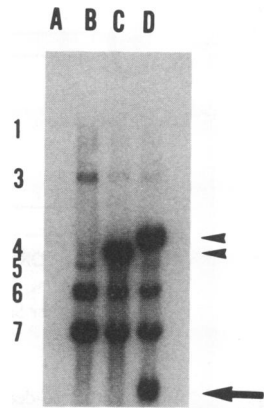

FIG. 4. Northern blot analysis of DI genomic RNA and subgenomic RNA. Virus-specific RNA species were separated on 1% formaldehyde gels and transferred to Biodyne nylon filters as described in Materials and Methods. The 5′-end-labeled oligonucleotide 79 was used as a probe. Passage 1 virus samples were used as virus inoculum. Lanes: A, mock-infected cells; B, MHV-A59-infected cells; C, MC 136-1 DI RNA replicating cells; D, PR6 DI RNA replicating cells. Numbers 1 to 7 represent the MHV-A59-specific mRNA species. DI genomic RNA and subgenomic RNA are shown by arrowheads and an arrow, respectively.

DIssF-derived DI cDNA clone, PR6, was constructed with an intergenic site, originating between genes 6 and 7, inserted at a new location downstream of the MHV packaging signal (Fig. 2). During the construction of PR6, another DI cDNA clone, PR7, with two intergenic regions was also obtained (Fig. 1). Plasmids PR6 and PR7 and their parent MC 136-1 were linearized with *Xba*I, transcribed by T7 RNA polymerase in the presence of a cap analog [$m^7G(5')ppp(5')G$] (18), and the resulting RNAs were transfected by lipofection into monolayers of DBT cells infected with MHV-A59 helper virus 1 h prior to transfection. After incubation of virus-infected cells at 37°C for 16 h, the culture fluid was harvested and the cell debris was removed by low-speed centrifugation. This sample was named passage 0 and was used for inoculation into fresh DBT cells to obtain a passage 1 virus sample. The passage 1 virus sample harvested after 16 h of culture was used as the inoculum for the analysis of intracellular RNA species. Virus-specific RNAs were labeled with $^{32}P_i$ in the presence of actinomycin D (25) and analyzed by agarose gel electrophoresis (Fig. 3). Efficient replication of MC 136-1, PR6, and PR7 genomic DI RNAs of expected sizes was detected. Furthermore, one MHV-specific RNA of 1.1 kb was clearly demonstrated in the cells infected with DI particles containing PR6 DI RNA. In PR7 replicating cells, two additional RNAs of 1.1 and 1.6 kb were demonstrated. The size of these RNA species was consistent with that of the predicted subgenomic DI RNA species containing leader sequence at the 5′ end and body sequence starting from the inserted intergenic site. Oligo(dT)-cellulose column chromatographic analysis demonstrated that all actinomycin D-resistant MHV-specific RNAs contain poly(A) sequences, most likely at the 3′ end (data not shown). The amount of synthesized DI genomic RNA in PR6 DI RNA-transfected cells was noticeably lower than that of DIssE (data not shown) (18).

Evidence of the synthesis of a subgenomic DI RNA. The structure of the PR6 1.1-kb RNA was examined to prove that it was indeed a subgenomic DI RNA species. The presence of the leader sequence in this RNA was examined by Northern blot analysis with synthetic oligonucleotide 79, which hybridizes with the positive-sense MHV leader sequence. As shown in Fig. 4, all MHV-specific RNA species, including the 1.1-kb RNA species, demonstrated the presence of the leader sequence. Next, the structure of the 1.1-kb RNA was examined by using S1 nuclease protection experiments. A gel-purified complete cDNA product of the 1.1-kb RNA was hybridized with an in vitro-synthesized PR6 DI RNA, and the RNA-DNA hybrid was treated with nuclease S1. The S1-resistant DNA fragment was then analyzed by glyoxal-agarose gel electrophoresis (Fig. 5). The S1 nuclease-resistant cDNA fragment migrated faster than the S1 nuclease-untreated cDNA sample, corresponding to a difference of about 70 to 80 nucleotides, indicating that the structures of the 1.1-kb RNA species and the PR6 DI genomic RNA were identical except for the 70- to 80-nucleotide region at the either end of the cDNA. The leader sequence is 72 to 77 nucleotides long (9); thus, most probably the S1 nuclease-susceptible 70 to 80 nucleotides came from the 5′ end leader sequence of 1.1-kb RNA. The structure of the 1.1-kb RNA species was further confirmed by an RNase protection assay in which in vitro-synthesized anti-sense RNA of the genomic PR6 DI RNA was mixed with the ^{32}P-labeled gel-purified 1.1-kb RNA species, and the RNA-RNA hybrids were treated with RNase A and RNase T_1 (28). A major RNase-resistant RNA species migrating slightly faster than the 1.1-kb RNA, again corresponding to about a 70- to 80-nucleotide difference, was demonstrated (data not shown). These data indicated that the sequence diversity between the 1.1-kb RNA and PR6 genomic RNA was at the 5′ end of the 1.1-kb RNA and further confirmed the results of the S1 nuclease assay. The structure of the

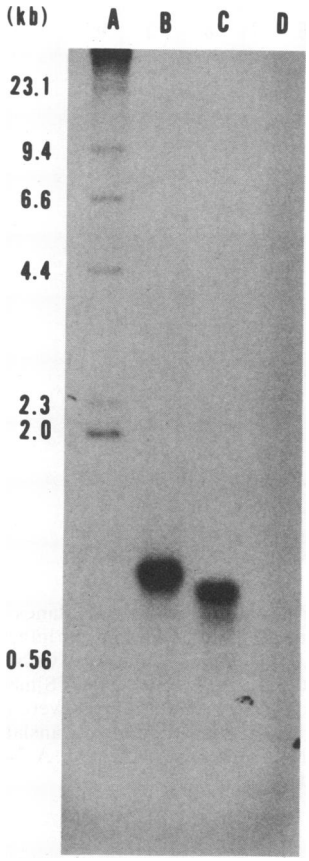

FIG. 5. S1 nuclease mapping analysis. ^{32}P-labeled complete cDNA of DI subgenomic RNA was hybridized with in vitro-synthesized PR6 DI RNA. The RNA-DNA hybrids were incubated with nuclease S1, and the nuclease resistant DNA was separated on a 1.4% agarose gel after denaturation with glyoxal. Lanes: A, marker DNA; B, DNA obtained from the RNA-DNA hybrid which was not incubated with S1 nuclease; C, DNA obtained from the RNA-DNA hybrid which was treated with S1 nuclease; D, DNA was incubated in the absence of RNA and then treated with S1 nuclease.

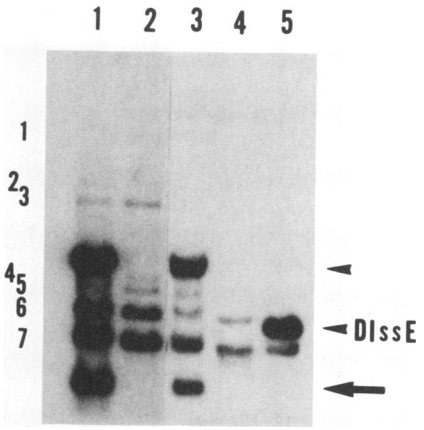

FIG. 6. Northern blot analysis of DI-specific RNA species. MHV-specific intracellular RNA species were examined by Northern blot analysis with oligonucleotide 79 as a probe. The in vitro-synthesized PR6 RNA (lane 1), gel-purified PR6 genomic DI RNA from PR6 replicating cells (lane 3), gel-purified subgenomic DI RNA from PR6 replicating cells (lane 4), and in vitro-synthesized DE25 RNA (DIssE clone [15]) (lane 5) were transfected into MHV-A59-infected cells, and passage 1 virus samples were prepared for virus inoculum. Lane 2, intracellular RNA species from MHV-A59-infected cells. Numbers 1 to 7 at the left side of gel represent MHV-specific mRNA species. DI genomic RNA and subgenomic DI RNA species are shown by an arrowhead and an arrow, respectively.

1.1-kb RNA was further examined by sequence analysis. First, the extreme 5′ end of the 1.1-kb RNA was sequenced using oligonucleotide 7 (22), complementary to nucleotides 87 to 104 from the 5′ end of mRNA 7 as a primer (34). The dideoxynucleotide chain termination method adapted for RNA sequencing was used (42). This result revealed that the 1.1-kb RNA contained the complete leader sequence in its 5′ end (data not shown). Second, the structure of the 1.1-kb RNA body sequence was examined by creating 1.1-kb RNA-specific cDNA clones by PCR. The first strand of cDNA was synthesized by incubating gel-purified 1.1-kb RNA with an oligo(dT)$_{12-18}$ primer followed by priming of second strand synthesis with oligonucleotide 78, which hybridizes with the negative sense of MHV leader sequence, under the PCR conditions described above. The predicted-size PCR product was cloned into a plasmid vector. Sequence analysis of the cDNA clone revealed that the body sequence of the 1.1-kb RNA was identical to the corresponding region of PR6 (data not shown).

In order to exclude the possibility that the 1.1-kb RNA species was a new genomic DI RNA species, the ability of the 1.1-kb RNA to replicate in the absence of PR6 genomic DI RNA was examined. Gel-purified PR6 DI RNA and the 1.1-kb RNA, both of which were extracted from virus-infected cells, were transfected independently into MHV-A59-infected cells. Normally, subsequent passages of virus samples obtained from DI RNA-transfected cells result in efficient amplification of DI particles (26); for this reason the virus from this transfected culture was also further passaged to obtain the passage 1 virus samples. The intracellular RNA was extracted from passage 1 virus-infected cells, and the presence of MHV-specific RNA species was confirmed by Northern blotting with oligonucleotide 79, which hybridizes specifically to the positive-sense leader sequence, as a probe (Fig. 6). Synthesis of the 1.1-kb RNA was not detected in cells infected with virus samples originally derived from the 1.1-kb RNA-transfected cells, whereas synthesis of both the 1.1-kb RNA and the genomic PR6 DI RNAs were demonstrated in cells infected with the virus derived from PR6 genomic DI RNA-transfected cells. Absence of the 1.1-kb RNA is not likely to be due to the absence of the packaging signal on the 1.1-kb RNA, because replication of DE25 DI RNA, which does not contain the packaging signal, was observed (18) (Fig. 6, lane 5). Furthermore, synthesis of the 1.1-kb RNA in MHV-A59-infected cells transfected with that RNA was also not detectable by $^{32}P_i$ labeling (data not shown). These studies unambiguously demonstrated that the 1.1-kb RNA species was a subgenomic DI RNA species which contained the leader sequence at the 5′ end and a body sequence starting from the inserted intergenic sequence.

The subgenomic DI RNA has a mRNA function. The structure of the PR6 subgenomic DI RNA species demonstrated that it has an open reading frame of 447 nucleotides (Fig. 2) corresponding to the N terminus of the MHV-JHM N protein. To examine whether the subgenomic DI RNA has an mRNA function, [^{35}S]methinone-labeled intracellular virus-specific proteins in the PR6 DI RNA replicating cells

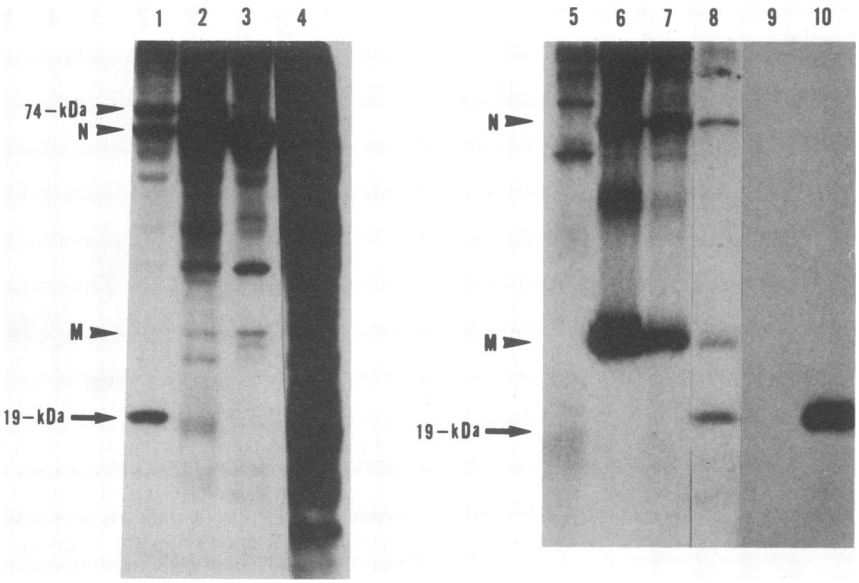

FIG. 7. Translation of the DI subgenomic RNA-specific protein. PAGE of proteins from virus-infected cells (lanes 1 to 8) and in vitro translation products in rabbit reticulocyte lysate (lanes 9 and 10). DBT cells were mock infected (lanes 4 and 5) or infected with MHV-A59 (lanes 3 and 6), with MHV-A59 obtained from MC 136-1 RNA-transfected cells (passage 1 virus) (lanes 2 and 7), or with MHV-A59 obtained from PR6 RNA-transfected cells (passage 1 virus) (lanes 1 and 8). At 8 h postinfection, cultures were labeled with [^{35}S]methionine for 15 min, and the cytoplasmic lysates were prepared and analyzed directly by SDS-PAGE (lanes 1 to 4). ^{35}S-labeled samples were immunoprecipitated with anti-MHV-JHM serum and analyzed by SDS-PAGE (lanes 5 to 10). Lanes 10 and 9 are ^{35}S-labeled in vitro translation products of the gel-purified subgenomic DI RNA and no RNA, respectively. MHV-A59-specific N and M proteins are indicated. A 74-kDa protein is the DIssF-specific protein (26). The subgenomic DI RNA-specific 19-kDa protein is indicated by arrows.

were examined by SDS-PAGE. A 19-kDa protein was specifically detected in PR6-replicating cells but not in MC 136-1 DI RNA replicating cells, MHV-A59-infected cells, and mock-infected cells (Fig. 7). This 19-kDa protein was immunoprecipitated with an anti-MHV-JHM serum (41) from cell extracts which were made from PR6 DI RNA replicating cells. The 19-kDa protein was also detected by immunoprecipitation of the PR6 subgenomic DI RNA in vitro translation product, isolated from virus-infected cells. The molecular mass of this protein is very close to the predicted molecular mass of 19,621 Da. Thus, it was concluded that the 19-kDa protein was specifically translated from the PR6 subgenomic DI RNA and that the subgenomic DI RNA had an mRNA function.

Effects of nucleotide deletions at the intergenic site on subgenomic DI RNA transcription. It has been demonstrated that the consensus sequence, UCUAAAC, at the intergenic sequence is important for MHV transcription (8, 33). A system which expresses subgenomic DI RNA from genomic DI RNA would be ideal for examining whether the sequence alterations at the consensus sequence affect MHV subgenomic mRNA synthesis. The present study focused on a stretch of 18 nucleotides (Fig. 8). This 18-nucleotide stretch is present twice in the MHV genomic sequence, once at the 3′ end of the leader sequence and once again at the intergenic sequence between genes 6 and 7 (Fig. 8) (33).

The DI RNAs synthesized in vitro from PR6 and nine PR6-derived deletion mutants were transfected into MHV-infected cells. The sequences of all mutants are shown in Fig. 8. Efficiency of DI genomic RNA and subgenomic DI RNA synthesis of each mutant in passage 1 virus-infected cells was examined by Northern blotting with oligonucleotide 79 as a probe (Fig. 9). The molar ratio of the subgenomic DI RNA to the DI genomic RNA was examined by densitometric scanning of the autoradiograms (Fig. 8). Deletions at the first 2 nucleotides (PR6 mutant 1) and the last 4 nucleotides (PR6 mutant 2) did not significantly affect the synthesis of subgenomic DI RNA, whereas deletion of both regions (PR6 mutant 8) significantly decreased the amount of subgenomic DI RNA synthesized. Removal of one UCUAA repeat within the 18 nucleotides resulted in a significant reduction in subgenomic DI RNA synthesis (PR6 mutant 9). Two additional A nucleotides deleted in PR6 mutant 9 did not affect the amount of subgenomic DI RNA synthesized (PR6 mutant 10), whereas the destruction of the second UCUAA sequence by the deletion of two A residues abolished subgenomic DI RNA synthesis (PR6 mutant 11). Because PR6 mutant 10 and PR6 mutant 11 contained the identical number and species of nucleotides deleted, this result indicated that the UCUAAAC sequence was indeed important for subgenomic mRNA synthesis. Interestingly, synthesis of subgenomic DI RNA was not observed in cells which were infected with PR6 mutant 3, which lacked all of the intergenic sequence except for the consensus sequence of UCUAAAC. Two additional mutants, PR6 mutants 4 and 5, both of which were deleted within the UCUAAAC sequence, also lost the ability to synthesize subgenomic DI RNA. The absence of subgenomic DI RNA in cells infected with PR6 mutants 3, 4, 5, and 11 was further confirmed by PCR in which MHV-specific cDNAs were first synthesized by using the intracellular RNA species in passage 1 virus-infected cells and oligonucleotide 130 as a primer. The cDNAs were mixed with oligonucleotide 78 (18), which hybridizes with anti-sense leader sequence. After 25 cycles of PCR, PCR products were analyzed by agarose gel electrophoresis. The PCR product of the predicted size was not detected in the sample obtained from the above-described passage 1 virus-infected cells, whereas the PCR product of

		Molar ratio, Subgenomic DI RNA/ Genomic DI RNA
Leader Sequence	UAAAACUCUUGUAGUUUAAAUCUAAUCUAAACUUUAUAAACGGCAC	
Intergenic Region	GGACACCGUAUUGUUGAGAAUCUAAUCUAAACUUUAAGGAUGUCUU	
mRNA 7	UAAAACUCUUGUAGUUUAAAUCUAAUCUAAACUUUAAGGAUGUCUU	
PR6	GGACACCGUAUUGUUGAGAAUCUAAUCUAAACUUUAAGGAUGUCUU	0.8
PR6-mutant 1	GGACACCGUAUUGUUGAG--UCUAAUCUAAACUUUAAGGAUGUCUU	0.7
PR6-mutant 9	GGACACCGUAUUGUUGAG-----AAUCUAAACUUUAAGGAUGUCUU	0.3
PR6-mutant 10	GGACACCGUAUUGUUGAG-------UCUAAACUUUAAGGAUGUCUU	0.3
PR6-mutant 11	GGACACCGUAUUGUUGAG-----AAUCUA--CUUUAAGGAUGUCUU	-
PR6-mutant 2	GGACACCGUAUUGUUGAGAAUCUAAUCUAAAC----AGGAUGUCUU	0.7
PR6-mutant 8	GGACACCGUAUUGUUGAG--UCUAAUCUAAAC----AGGAUGUCUU	0.3
PR6-mutant 3	GGACACCGUAUUGUUGAG-------UCUAAAC----AGGAUGUCUU	-
PR6-mutant 4	GGACACCGUAUUGUUGAG-------UCUAAA-----AGGAUGUCUU	-
PR6-mutant 5	GGACACCGUAUUGUUGAG--------CUAAAC----AGGAUGUCUU	-

FIG. 8. Sequence comparison of the leader sequence, intergenic region between genes 6 and 7, mRNA 7, and PR6-derived mutant DI RNAs. The sequences at the intergenic sites are presented in plus sense. The regions of homology with the 3′ end leader RNA and the intergenic site are underlined by a thin line. A bold solid line represents the nine-nucleotide sequence which is deleted in certain MHV strains (22) but present in MHV-A59. Sequences missing in the PR6-derived mutants are shown by dashes. The molar ratios of genomic DI RNA to subgenomic DI RNA is the average of three independent experiments.

the predicted size was clearly demonstrated in the sample obtained from PR6 mutant 8-infected cells (data not shown). These data thus demonstrated that the presence of UCU AAAC was necessary but not sufficient for the synthesis of subgenomic DI RNA species.

DISCUSSION

In the present study it was demonstrated that a subgenomic DI RNA was transcribed from DI genomic RNA into which an intergenic sequence had been inserted. The struc-

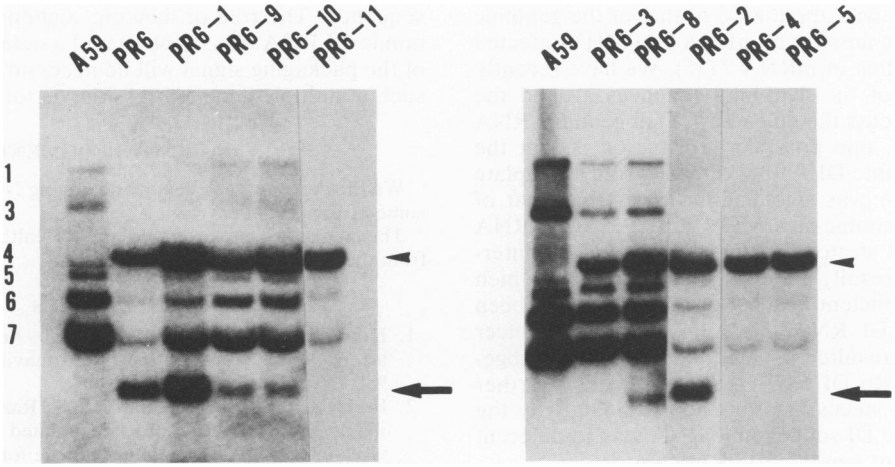

FIG. 9. Northern blot analysis of subgenomic DI RNA species of PR6-derived mutants. Passage 1 virus samples were used for virus inoculum. Intracellular RNAs were extracted 7 h postinfection, separated by 1% formaldehyde gel electrophoresis and transferred to nylon membrane. The 5′-end-labeled oligonucleotide 79 was used as a probe. PR6-1, PR6-9, PR6-10, PR6-11, PR6-3, PR6-8, PR6-2, PR6-4, and PR6-5 represent PR6 mutant 1, PR6 mutant 9, PR6 mutant 10, PR6 mutant 11, PR6 mutant 3, PR6 mutant 8, PR6 mutant 2, PR6 mutant 4, and PR6 mutant 5, respectively. Numbers 1 to 7 represent MHV-A59-specific mRNA species. DI genomic RNAs and subgenomic DI RNAs are shown by arrowheads and arrows, respectively.

ture of the subgenomic DI RNA, capable of forming the coronavirus-specific unique 3'-coterminal nested-set structure, was unambiguously demonstrated by oligo(dT) column chromatography, Northern blotting, sequence analysis, RNase protection analysis, and S1 nuclease mapping. Transfection of the PR6 genomic DI RNA into MHV-infected cells clearly demonstrated that genomic DI RNA was sufficient for subgenomic DI RNA synthesis. This result was consistent with the previous observation that only genomic RNA is detected in purified MHV virion (13, 20). Therefore, MHV subgenomic mRNA synthesis must undergo a step in which the positive sense or negative sense of genomic MHV RNA serves as template RNA for the subgenomic mRNA.

The presence of negative-strand subgenomic RNAs containing anti-leader sequence leads to the proposal that subgenomic mRNA synthesis may involve the replication of each subgenomic mRNA species (30, 31). In the present study, replication of transfected subgenomic DI RNA into MHV-infected cells was not observed. We have observed that negative-strand subgenomic DI RNA was present in PR6 DI RNA replicating cells and that two DI RNA-specific replicative-form RNAs, one corresponding to the PR6 genomic DI RNA and one to the subgenomic DI RNA, are generated after RNase treatment of intracellular RNA species extracted from PR6 DI RNA replicating cells (data not shown). Therefore, it seems that subgenomic DI RNA synthesis undergoes processes identical to those used for infectious virus mRNA synthesis. If the subgenomic mRNA indeed accumulates via amplification, then why was replication of the transfected subgenomic DI RNA not observed? It is possible that in order to start mRNA amplification, mRNA species must be synthesized de novo from template RNA in transcriptional complexes, and the mRNA associated with this complex may then be further amplified. We have observed that relatively large amounts of transfected subgenomic DI RNAs were not degraded even as late as 10 h posttransfection in MHV-infected cells (7). This makes it likely that input subgenomic DI RNA was very much present throughout infection. Therefore, if mRNA amplification activities are synthesized only late in infection, then transfected subgenomic DI RNA would not have been likely to be degraded before such activities accumulated.

It is interesting to note that the amount of PR6-derived subgenomic DI RNA was about 80% of that of the genomic DI RNA, whereas the amount of mRNA 1 in MHV-infected cells is only 1.5% of that of mRNA 7 (15). We have recently found that deletion of the flanking sequences around the intergenic region affected the efficiency of subgenomic RNA synthesis (16). Thus, one possible explanation is that the efficiency of subgenomic DI RNA synthesis from a template genome-size DI RNA was significantly lower than that of mRNA 7 from the genome-size MHV RNA. PR6 DI RNA contains only a short stretch of sequence around the intergenic region and as a result, some enhancer sequences which are important for efficient transcription may have been missing in the PR6 DI RNA. Deletion of such enhancer sequences may have resulted in accumulation of less subgenomic DI RNA in PR6 DI RNA replicating cells. Further studies are obviously necessary for understanding why the ratio of DI genomic to DI subgenomic RNA was so different from that of the parent genome to its mRNA.

The data obtained from the analysis of deletion mutants demonstrated that the consensus sequence present in the intergenic sequence was indeed important for MHV RNA transcription. This conclusion was derived from the comparison of PR6 mutant 10 and PR6 mutant 11, both of which have deletions consisting of the same number of nucleotides. PR6 mutant 10 supported efficient subgenomic DI RNA synthesis, whereas no subgenomic DI RNA was synthesized from PR6 mutant 11. Analysis of PR6 mutant 3 indicated that the presence of the consensus sequence, UCUAAAC, was not sufficient for subgenomic DI RNA synthesis, indicating that other regions also may be important for subgenomic mRNA synthesis. The effect of the deletion of UUUA was also considerably interesting. We have previously isolated mutant MHVs which have a deletion of 9 nucleotides (UUUAUAAAC) at the 3' region of the leader sequence at the genomic RNA (Fig. 8, sequence with a bold underline) and these mutant MHVs synthesize essentially the same amount of mRNA 7 as does wild-type MHV (22, 25). Therefore, it seems that the UUUA sequence homology between leader sequence and the intergenic sequence may not be important for the efficiency of transcription. The present data indeed demonstrated that deletion of UUUA did not significantly affect subgenomic mRNA synthesis (PR6 and PR6 mutant 2). Interestingly, deletion of two A's upstream of the consensus sequence did not affect the transcriptional efficiency (PR6 mutant 1), whereas deletion of both A's and UUUA at the intergenic sequence did (PR6 mutant 8). These data suggest that the UUUA sequence was also involved in the regulation of mRNA synthesis under certain circumstances, e.g., deletion or sequence alteration of another region(s). It seems that the sequence around the consensus sequence and/or the secondary structure made by the consensus sequence and the flanking sequences were important for the regulation of transcription efficiency. Alternatively, these results may indicate that subgenomic DI RNA transcription may be affected by changes in the distance of the consensus sequence relative to its flanking sequences. This is the first direct demonstration that the sequences flanking the consensus sequence play an important role in the regulation of coronavirus transcription.

The subgenomic DI RNA functioned as an mRNA, and two subgenomic DI RNAs resulted from the insertion of two intergenic regions into the DI RNA template. Therefore, it is possible that this MHV DI subgenomic RNA system can be developed as an expression vector in which multiple subgenomic DI RNAs are expressed, and regulation of that expression can be controlled by alteration of the intergenic sequence. The role of flanking sequence in efficient subgenomic DI RNA transcription and a detailed characterization of the packaging signal will be necessary for development of such a multiple gene expression vector.

ACKNOWLEDGMENTS

We thank Yong Seok Jeong and Young Nam Kim for performing some of the preliminary work.

This work was supported by Public Health Service grant AI29984 from the National Institutes of Health.

REFERENCES

1. **Baker, S. C., and M. M. C. Lai.** 1990. An in vitro system for the leader-primed transcription of coronavirus mRNAs. EMBO J. **9**:4173–4179.
2. **Baric, R. S., S. A. Stohlman, M. K. Razavi, and M. M. C. Lai.** 1985. Characterization of leader-related small RNAs in coronavirus-infected cells: further evidence for leader-primed mechanism of transcription. Virus Res. **3**:19–33.
3. **Felgner, P. L., T. R. Gadek, M. Holm, R. Roman, H. W. Chan, M. Wenz, J. P. Northrop, G. M. Ringgold, and M. Danielson.** 1987. Lipofection: a highly efficient, lipid-mediated DNA-transfection procedure. Proc. Natl. Acad. Sci. USA **84**:7413–7417.
4. **Fosmire, J. A., and S. Makino.** Unpublished data.

5. **Higuchi, R.** 1990. Recombinant PCR, p. 177–183. *In* M. A. Innis, D. H. Gelfand, J. J. Sninsky, and T. J. White (ed.), PCR protocols. Academic Press, Inc., San Diego.
6. **Hirano, N., K. Fujiwara, S. Hino, and M. Matsumoto.** 1974. Replication and plaque formation of mouse hepatitis virus (MHV-2) in mouse cell line DBT culture. Arch. Gesamte Virusforch. **44**:298–302.
7. **Jeong, Y. S., and S. Makino.** Unpublished data.
8. **Lai, M. M. C.** 1990. Coronavirus: organization, replication and expression of genome. Annu. Rev. Microbiol. **44**:303–333.
9. **Lai, M. M. C., R. S. Baric, P. R. Brayton, and S. A. Stohlman.** 1984. Characterization of leader RNA sequences on the virion and mRNAs of mouse hepatitis virus, a cytoplasmic RNA virus. Proc. Natl. Acad. Sci. USA **81**:3626–3630.
10. **Lai, M. M. C., P. R. Brayton, R. C. Armen, C. D. Patton, C. Pugh, and S. A. Stohlman.** 1981. Mouse hepatitis virus A59: mRNA structure and genetic localization of the sequence divergence from hepatotropic strain MHV-3. J. Virol. **39**:823–834.
11. **Lai, M. M. C., C. D. Patton, R. S. Baric, and S. A. Stohlman.** 1983. Presence of leader sequences in the mRNA of mouse hepatitis virus. J. Virol. **46**:1027–1033.
12. **Lai, M. M. C., C. D. Patton, and S. A. Stohlman.** 1982. Replication of mouse hepatitis virus: negative-stranded RNA and replicative form RNA are of genomic length. J. Virol. **44**:487–492.
13. **Lai, M. M. C., and S. A. Stohlman.** 1978. RNA of mouse hepatitis virus. J. Virol. **26**:236–242.
14. **Lee, H.-J., C.-K. Shieh, A. E. Gorbalenya, E. V. Eugene, N. La Monica, J. Tuler, A. Bagdzhadzhyan, and M. M. C. Lai.** 1991. The complete sequence (22 kilobases) of murine coronavirus gene 1 encoding the putative proteases and RNA polymerase. Virology **180**:567–582.
15. **Leibowitz, J. L., K. C. Wilhelmsen, and C. W. Bond.** 1981. The virus-specific intracellular RNA species of two murine coronaviruses: MHV-A59 and MHV-JHM. Virology **114**:39–51.
16. **Makino, S.** Unpublished data.
17. **Makino, S., N. Fujioka, and K. Fujiwara.** 1985. Structure of the intracellular defective viral RNAs of defective interfering particles of mouse hepatitis virus. J. Virol. **54**:329–336.
18. **Makino, S., and M. M. C. Lai.** 1989. High-frequency leader sequence switching during coronavirus defective interfering RNA replication. J. Virol. **63**:5285–5292.
19. **Makino, S., and M. M. C. Lai.** 1989. Evolution of the 5′-end of genomic RNA of murine coronaviruses during passages in vitro. Virology **169**:227–232.
20. **Makino, S., C.-K. Shieh, J. G. Keck, and M. M. C. Lai.** 1988. Defective-interfering particles of murine coronaviruses: mechanism of synthesis of defective viral RNAs. Virology **163**:104–111.
21. **Makino, S., C.-K. Shieh, L. H. Soe, S. C. Baker, and M. M. C. Lai.** 1988. Primary structure and translation of a defective interfering RNA of murine coronavirus. Virology **166**:550–560.
22. **Makino, S., L. H. Soe, C.-K. Shieh, and M. M. C. Lai.** 1988. Discontinuous transcription generates heterogeneity at the leader fusion sites of coronavirus mRNAs. J. Virol. **62**:3870–3873.
23. **Makino, S., S. A. Stohlman, and M. M. C. Lai.** 1986. Leader sequences of murine coronavirus mRNAs can be freely reassorted: evidence for the role of free leader RNA in transcription. Proc. Natl. Acad. Sci. USA **83**:4204–4208.
24. **Makino, S., F. Taguchi, and K. Fujiwara.** 1984. Defective interfering particles of mouse hepatitis virus. Virology **133**:9–17.
25. **Makino, S., F. Taguchi, N. Hirano, and K. Fujiwara.** 1984. Analysis of genomic and intracellular viral RNAs of small plaque mutants of mouse hepatitis virus, JHM strain. Virology **139**:138–151.
26. **Makino, S., K. Yokomori, and M. M. C. Lai.** 1990. Analysis of efficiently packaged defective interfering RNAs of murine coronavirus: localization of a possible RNA-packaging signal. J. Virol. **64**:6045–6053.
27. **McMaster, G. K., and G. G. Carmichael.** 1977. Analysis of single- and double-stranded nucleic acids on polyacrylamide and agarose gels by using glyoxal and acridine orange. Proc. Natl. Acad. Sci. USA **74**:4835–4838.
28. **Sambrook, J., E. F. Fritsch, and T. Maniatis.** 1989. Molecular cloning: a laboratory manual, 2nd ed. Cold Spring Harbor Laboratory, Cold Spring Harbor, N.Y.
29. **Sawicki, S. G., and D. L. Sawicki.** 1990. Coronavirus transcription: subgenomic mouse hepatitis virus replicative intermediates function in RNA synthesis. J. Virol. **64**:1050–1056.
30. **Sethna, P. B., M. A. Hofmann, and D. A. Brian.** 1991. Minus-strand copies of replicating coronavirus mRNAs contain antileaders. J. Virol. **65**:320–325.
31. **Sethna, P. B., S.-L. Hung, and D. A. Brian.** 1989. Coronavirus subgenomic minus-strand RNAs and the potentional for mRNA replicons. Proc. Natl. Acad. Sci. USA **86**:5626–5630.
32. **Shieh, C.-K., H.-J. Lee, K. Yokomori, N. La Monica, S. Makino, and M. M. C. Lai.** 1989. Identification of a new transcriptional initiation site and the corresponding functional gene 2b in the murine coronavirus RNA genome. J. Virol. **63**:3729–3736.
33. **Shieh, C.-K., L. H. Soe, S. Makino, M.-F. Chang, S. A. Stohlman, and M. M. C. Lai.** 1987. The 5′-end sequence of the murine coronavirus genome: implications for multiple fusion sites in leader-primed transcription. Virology **156**:321–330.
34. **Skinner, M. A., and S. G. Siddell.** 1983. Coronavirus JHM: nucleotide sequence of the mRNA that encodes nucleocapsid protein. Nucleic Acid Res. **15**:5045–5054.
35. **Soe, L. H., C.-K. Shieh, S. C. Baker, M.-F. Chang, and M. M. C. Lai.** 1987. Sequence and translation of the murine coronavirus 5′-end genomic RNA reveals the N-terminal structure of the putative RNA polymerase. J. Virol. **61**:3968–3976.
36. **Spaan, W., H. Delius, M. Skinner, J. Armstrong, P. Rottier, S. Smeekens, B. A. M. van der Zeijst, and S. G. Siddell.** 1983. Coronavirus mRNA synthesis involves fusion of non-contiguous sequences. EMBO J. **2**:1939–1944.
37. **Stohlman, S. A., and M. M. C. Lai.** 1979. Phosphoproteins of murine hepatitis virus. J. Virol. **32**:672–675.
38. **Sturman, L. S., K. V. Holmes, and J. Behnke.** 1980. Isolation of coronavirus envelope glycoproteins and interaction with the viral nucleocapsid. J. Virol. **33**:449–462.
39. **van der Most, R. G., P. J. Bredenbeek, and W. J. M. Spaan.** 1991. A domain at the 3′ end of the polymerase gene is essential for encapsidation of coronavirus defective interfering RNAs. J. Virol. **65**:3219–3226.
40. **Weiss, B., H. Nitschko, I. Ghattas, R. Wright, and S. Schlesinger.** 1989. Evidence for specificity in the encapsidation of Sindbis virus RNAs. J. Virol. **63**:5310–5318.
41. **Yokomori, K., N. La Monica, S. Makino, C.-K. Shieh, and M. M. C. Lai.** 1989. Biosynthesis, structure, and biological activities of envelope protein gp65 of murine coronavirus. Virology **173**:683–691.
42. **Zimmern, D., and P. Kaesburg.** 1978. 3′-Terminal nucleotide sequence of encephalomyocarditis virus RNA determined by reverse transcriptase and chain terminating inhibitors. Proc. Natl. Acad. Sci. USA **75**:4257–4261.